Supplementary Material

Manuscript title:

Lipid droplets control mitogenic lipid mediator production in human cancer cells

Authors:

Eva Jarc Jovičić[1,2], Anja Pucer Janež[1,2], Thomas O. Eichmann[3,4], Špela Koren[1,2], Vesna Brglez[1,2], Paul M. Jordan[5], Jana Gerstmeier[5], Duško Lainšček[6,7], Anja Golob-Urbanc[6], Roman Jerala[6,7], Gérard Lambeau[8], Oliver Werz[5], Robert Zimmermann[3,9], and Toni Petan[1,*]

Contents:

Supplementary Figures 1–8

Supplementary Figure Legends

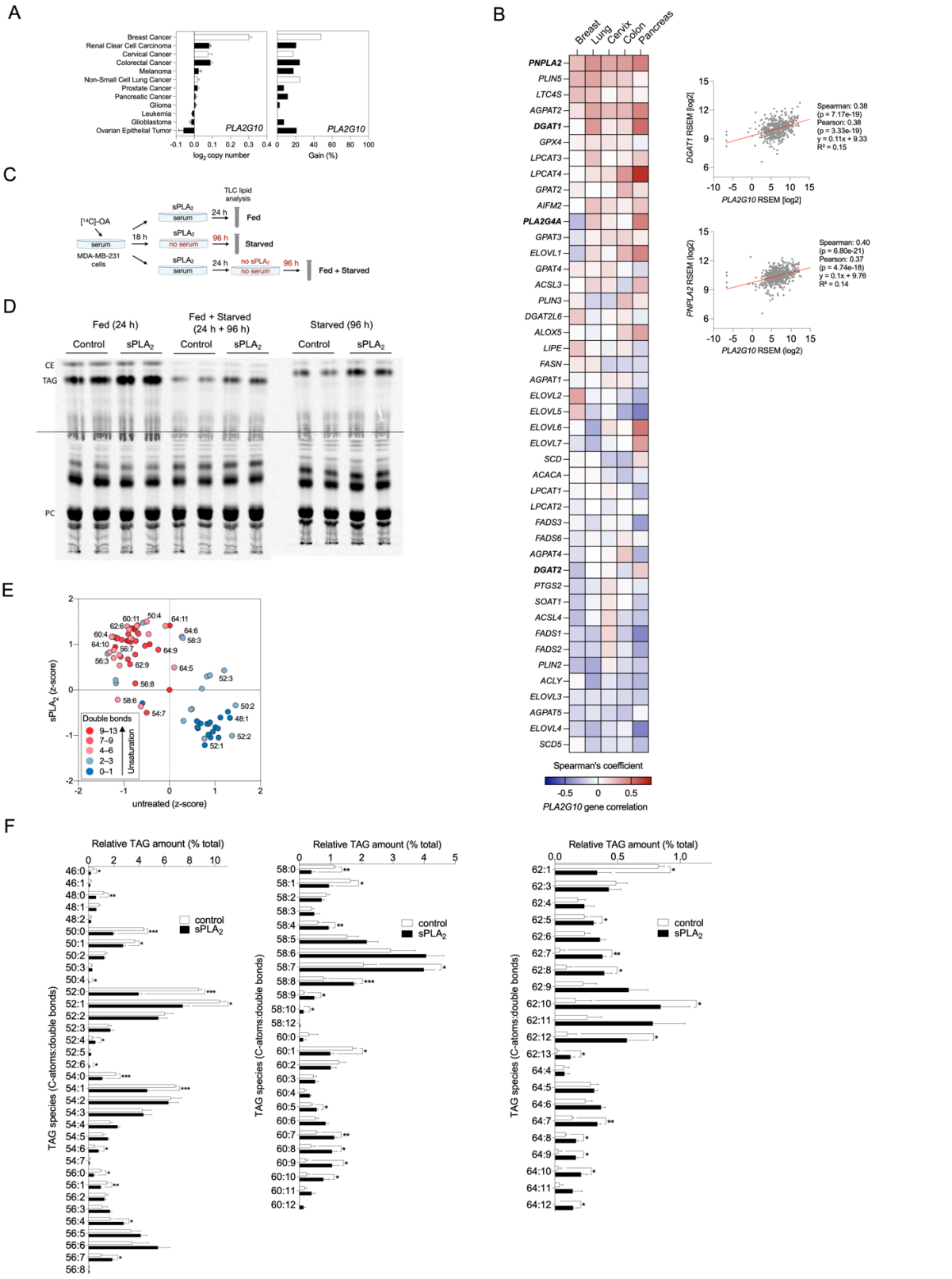

Supplementary Figure 1. *PLA2G10* gene alterations in cancer and group X sPLA$_2$-induced changes in LD metabolism and composition. (A) *PLA2G10* gene copy number and gain in copy number in samples of cancer patients (TCGA PanCancer Atlas Studies, cBioportal). Gain (%) refers to the percentage increase in the number of gene amplifications beyond the diploid copy number. (**B**) Heat map showing correlations between mRNA levels of *PLA2G10* and selected lipid metabolism genes in different cancer types (TCGA PanCancer Atlas Studies, cBioportal). Gene correlation was determined with Spearman's rank correlation coefficient. Graphs show pairwise correlations between *PLA2G10* and *DGAT1* or *PNPLA2* mRNA levels in lung adenocarcinoma samples. (**C**) Diagram illustrating the experimental set-up for oleate incorporation analyses shown in (D) and in Figure 1E. (**D**) Representative thin layer chromatography (TLC) plate showing oleate incorporation into TAGs, phosphatidylcholine (PC) or cholesterol esters (CE). (**E, F**) Lipidomic analysis of hGX-sPLA$_2$-induced PUFA-TAG enrichment in MDA-MB-231 cells grown under serum-rich conditions. (E) Representative XY z-score plot showing colour-coded changes in the levels of TAG acyl-chain unsaturation. Data are means ±SEM of three or four (F) independent experiments. *, P < 0.05; **, P < 0.01; ***, P < 0.001 (unpaired t-tests (F)).

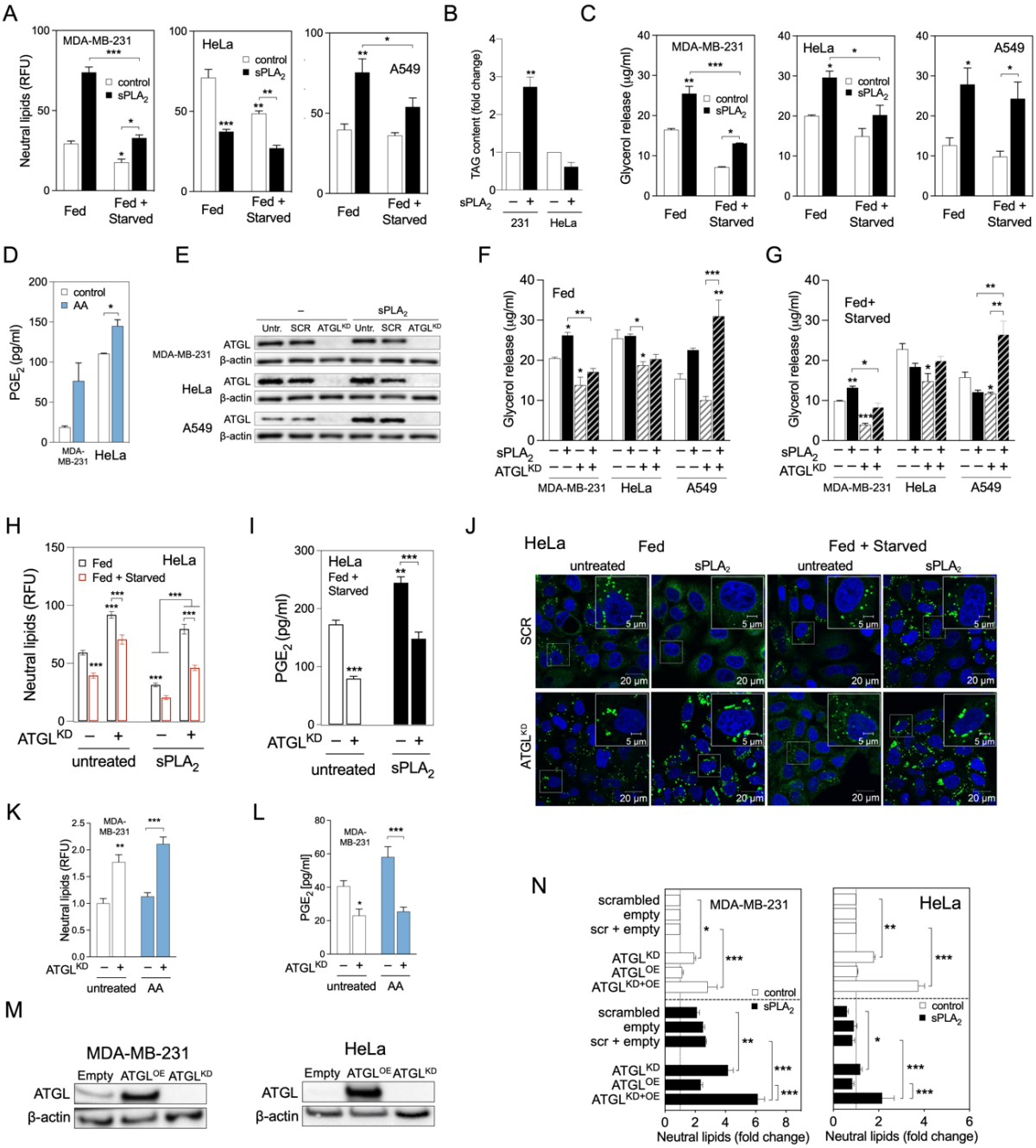

Supplementary Figure 2. ATGL-mediated LD breakdown drives PGE_2 production. (**A**) Neutral lipid contents in control and hGX-$sPLA_2$-treated cells at the beginning of and after serum starvation. (**B**) Total cellular triglycerides (TAGs) in control and hGX-$sPLA_2$-treated MDA-MB-231 and HeLa cells quantified using a biochemical assay. (**C**) Glycerol released from fed and starving control and hGX-$sPLA_2$-treated cells. (**D**) PGE_2 levels in cell supernatants of control and arachidonic acid (AA)-treated cells. (**E**) Representative western blot showing siRNA-induced ATGL knock down ($ATGL^{KD}$) in comparison with control (untransfected [untr.] and non-targeting siRNA-transfected [SCR] cells), treated and grown as shown in Fig. 2C. (**F, G**) Glycerol released in cell supernatants of control and ATGL-depleted serum-fed and serum-starved cells, either untreated or treated with hGX $sPLA_2$. (**H, I**) Neutral lipid and PGE_2 levels in ATGL-silenced control and $sPLA_2$-treated cells grown and analysed as shown in Fig. 2C. (**J**) Representative confocal microscopy images showing effects of ATGL depletion on cellular LD content in control and hGX-$sPLA_2$-treated cells, under serum-rich (Fed) and serum-free (Fed + Starved) conditions. LDs and nuclei were stained using BODIPY 493/503 and Hoechst 33342, respectively. (**K, L**) Changes in LD levels and PGE_2 production induced by ATGL silencing in control and AA-treated cells analysed as shown in Fig. 2C. (**M**) Representative western blot showing ATGL protein overexpression in cells transfected with ATGL-encoding plasmid ($ATGL^{OE}$) in comparison with those transfected with control (Empty) vector or ATGL-specific siRNA ($ATGL^{KD}$), grown as illustrated in Fig. 2L. (**N**) Neutral lipid levels in ATGL-overexpressing in untreated and hGX-$sPLA_2$-pretreated serum-starved cells, in comparison with those co-transfected with ATGL-specific siRNA ($ATGL^{KD+OE}$), non-targeting siRNA (scrambled) and control plasmid (empty), grown as shown in Fig. 2L. (A, H, K, N) Neutral lipids were quantified by Nile Red staining and flow cytometry. (D, I, L) PGE_2 was quantified by ELISA at the end of starvation. Data are means ±SEM of two (D) or three (A–C, F–I, K, L, N) independent experiments. *, $P < 0.05$; **, $P < 0.01$; ***, $P < 0.001$ (two-way ANOVA with Bonferroni (B, F–I, K, L) or Tukey (A, C, N) adjustment; unpaired t-test (D)).

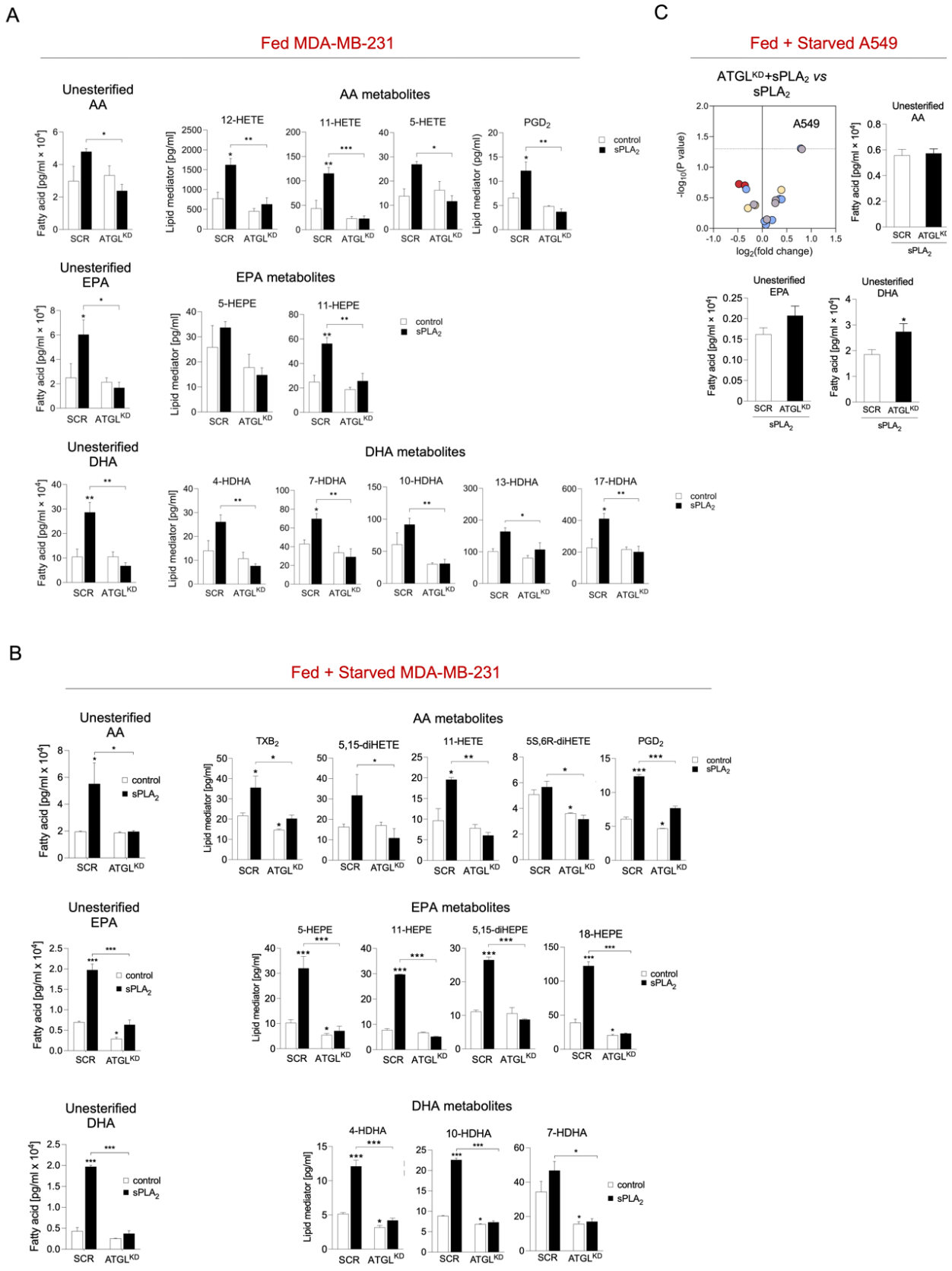

Supplementary Figure 3. Depletion of ATGL suppresses both basal and hGX-sPLA$_2$-stimulated lipid mediator production in fed and in starved cancer cells. (A, B) hGX-sPLA$_2$-induced and ATGL knockdown (ATGL^{KD})-induced changes in selected lipid mediators (as indicated) released from fed and fed plus starved MDA-MB-231 cells and analysed by UPLC-MS-MS. (**C**) Lipid mediators and fatty acids released from wild-type and ATGL-depleted serum-starved A549 cells pre-treated during feeding with hGX sPLA$_2$, presented as a volcano plot and graphs for selected individual species. Data are means ±SEM of three independent experiments. *, P < 0.05; **, P < 0.01; ***, P < 0.001 (two-way ANOVA with Sidak adjustment (A, B); unpaired t-test (C)). AA, arachidonic acid; DHA, docosahexaenoic acid; EPA, eicosapentaenoic acid; HDHA, hydroxydocosahexaenoic acid; HEPE, hydroxyeicosapentaenoic acid; HETE, hydroxyeicosatetraenoic acid; PGD$_2$, prostaglandin D$_2$; PGE$_2$, prostaglandin E$_2$; TXB$_2$, thromboxane B$_2$.

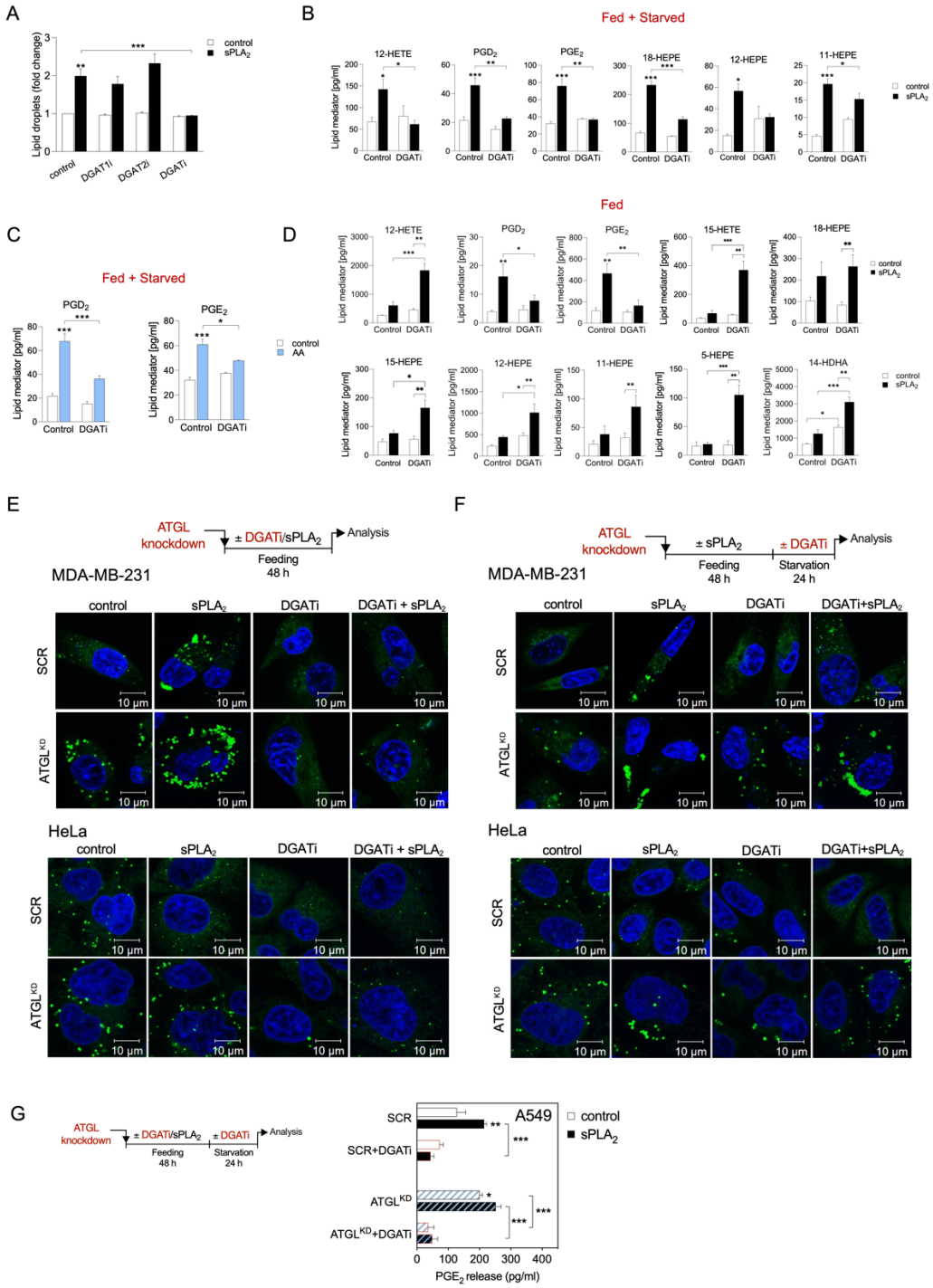

Supplementary Figure 4. Lipid mediator production induced by hGX sPLA$_2$ or exogenous AA depends on DGAT-mediated LD biogenesis. (**A**) Neutral lipid content in MDA-MB-231 cells grown in the absence and presence of T863 (DGAT1i) and PF-06427878 (DGAT2i), or an equimolar mix of both DGAT inhibitors (DGATi), without and with stimulation of LD biogenesis by hGX sPLA$_2$ during serum sufficiency. (**B**) hGX-sPLA$_2$-induced and DGAT inhibition (DGATi)-induced changes in selected lipid mediators (as indicated) released from serum-starved MDA-MB-231 cells. Cells were treated as shown in Figure 4A. (**C**) AA-induced and DGATi-induced changes in selected lipid mediators (as indicated). Cells were treated as shown in Figure 4A. (**D**) hGX-sPLA$_2$-induced and DGAT inhibition (DGATi)-induced changes in selected lipid mediators (as indicated) released from fed MDA-MB-231 cells. (**E, F**) Diagrams illustrating the experimental conditions used (top) and representative live-cell confocal microscopy images of control (SCR) and ATGL-depleted (ATGL^{KD}) MDA-MB-231 and HeLa cells treated with DGAT inhibitors during serum feeding (E) and during serum starvation (F), without and with hGX sPLA$_2$ pre-treatment. LDs and nuclei were visualised using BODIPY 493/503 and Hoechst 33342 staining and confocal microscopy. (**G**) Diagram illustrating the experimental conditions (left) and graph showing DGAT inhibition (DGATi)-induced changes in PGE$_2$ production in serum-starved control (SCR) and ATGL-depleted (ATGL^{KD}) A549 cells, without and with stimulation of LD biogenesis by hGX sPLA$_2$ pre-treatment. Neutral lipids were measured at the end of starvation with Nile Red staining and flow cytometry. Lipid mediators were quantified by UPLC-MS-MS. (G) PGE$_2$ levels were determined in cell supernatants as described in Methods. Data are means ±SEM of three (A, D) or four (B, C) independent experiments. *, P < 0.05; **, P < 0.01; ***, P < 0.001 (two-way ANOVA with Tukey (A), Sidak (B–D) or Bonferroni (G) adjustment). AA, arachidonic acid; DHA, docosahexaenoic acid; EPA, eicosapentaenoic acid; HDHA, hydroxydocosahexaenoic acid; HEPE, hydroxyeicosapentaenoic acid; HETE, hydroxyeicosatetraenoic acid; PGD$_2$, prostaglandin D$_2$; PGE$_2$, prostaglandin E$_2$; TXB$_2$, thromboxane B$_2$.

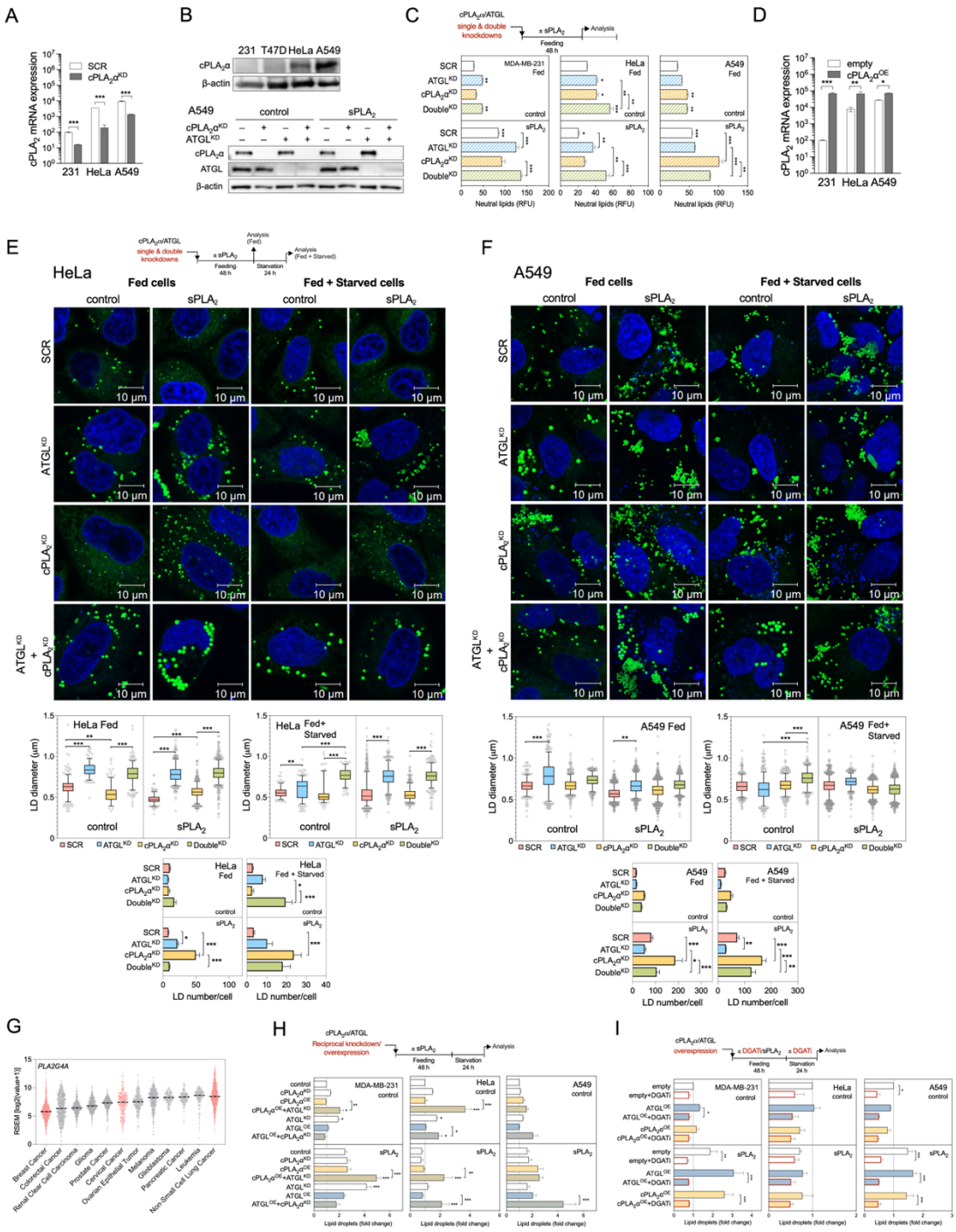

Supplementary Figure 5. cPLA₂α cooperates with ATGL in mediating LD-driven lipid mediator production. (**A**) Quantitative PCR analysis of cPLA₂α gene expression in control (SCR) and cPLA₂-knockdown (cPLA₂α^{KD}) cells grown for 48 h in complete medium and serum starved for 24 h. (**B**) Representative western blots showing basal levels of cPLA₂α protein expression in the four cancer cell lines (top) and cPLA₂α and ATGL protein expression in single and double knockdown A549 cells, without and with hGX sPLA₂ pre-treatment (bottom). (**C**) Diagram illustrating the experimental conditions used (top), and changes in neutral lipid content in serum-fed cells induced by ATGL (ATGL^{KD}) and cPLA₂α (cPLA₂α^{KD}) single and double (Double^{KD}) knockdowns, in comparison with control siRNA-treated cells (SCR), without and with stimulation of LD biogenesis by hGX sPLA₂ treatment. (**D**) Quantitative PCR analysis of cPLA₂α gene expression in control (empty) and cPLA₂α-overexpressing (cPLA₂α^{OE}) cells grown for 48 h in complete medium and serum starved for 24 h. (**E, F**) Diagram illustrating the experimental conditions used, representative live-cell confocal microscopy images and image analysis of LDs in ATGL (ATGL^{KD}) and cPLA₂α (cPLA₂α^{KD}) single and double (Double^{KD}) knockdown HeLa and A549 cells, in comparison with non-targeting control siRNA-treated cells (SCR), without and with stimulation of LD biogenesis by hGX sPLA₂ pre-treatment. LDs were stained with BODIPY 493/503 (green) and nuclei with Hoechst 33342 (blue) and images analysed using ImageJ and the LD Counter Plugin. Box plots are showing changes in LD diameters and LD numbers per cell in serum-fed (Fed) and serum-starved (Starved) cells. Data are geometric means (diameter analysis) or means (number analysis) ±SEM (n >40 cells/sample) of two independent experiments. (**G**) *PLA2G4A* mRNA expression in samples from cancer patients (TCGA PanCancer Atlas Studies, cBioportal). mRNA levels were batch normalized from Illumina HiSeq_RNASeqV2. Dashed line indicates median. (**H**) Diagram illustrating the experimental conditions used (top), and neutral lipid levels in cells with reciprocal knockdown/overexpression of cPLA₂α and ATGL. Cells were reverse transfected with ATGL-targeting (ATGL^{KD}) and/or cPLA₂α-targeting (cPLA₂α^{KD}) siRNAs, then forward transfected with ATGL-encoding (ATGL^{OE}) and/or cPLA₂α-encoding

($cPLA_2\alpha^{OE}$) plasmids, and/or pre-treated with hGX $sPLA_2$. In controls (control), non-targeting siRNA reverse transfections were combined with backbone ('empty') vector forward transfections. (**I**) Diagram illustrating the experimental conditions used (top), and DGAT inhibition (DGATi)-induced changes in neutral lipids in serum-starved control cells (empty) and in cells overexpressing ATGL ($ATGL^{OE}$) or $cPLA_2\alpha$ ($cPLA_2\alpha^{OE}$), without and with additional stimulation of LD biogenesis by hGX $sPLA_2$ pre-treatment. Neutral lipid content was quantified by Nile Red staining and flow cytometry. Data are means ±SEM of two (A, D; C, A549 cells) or at least three independent experiments. *, P < 0.05; **, P < 0.01; ***, P < 0.001 (unpaired t-tests (A, D); two-way ANOVA with Tukey (C, E, F, H) or Dunnet (I) adjustments; nested one-way ANOVA with Sidak adjustment (E, F)).

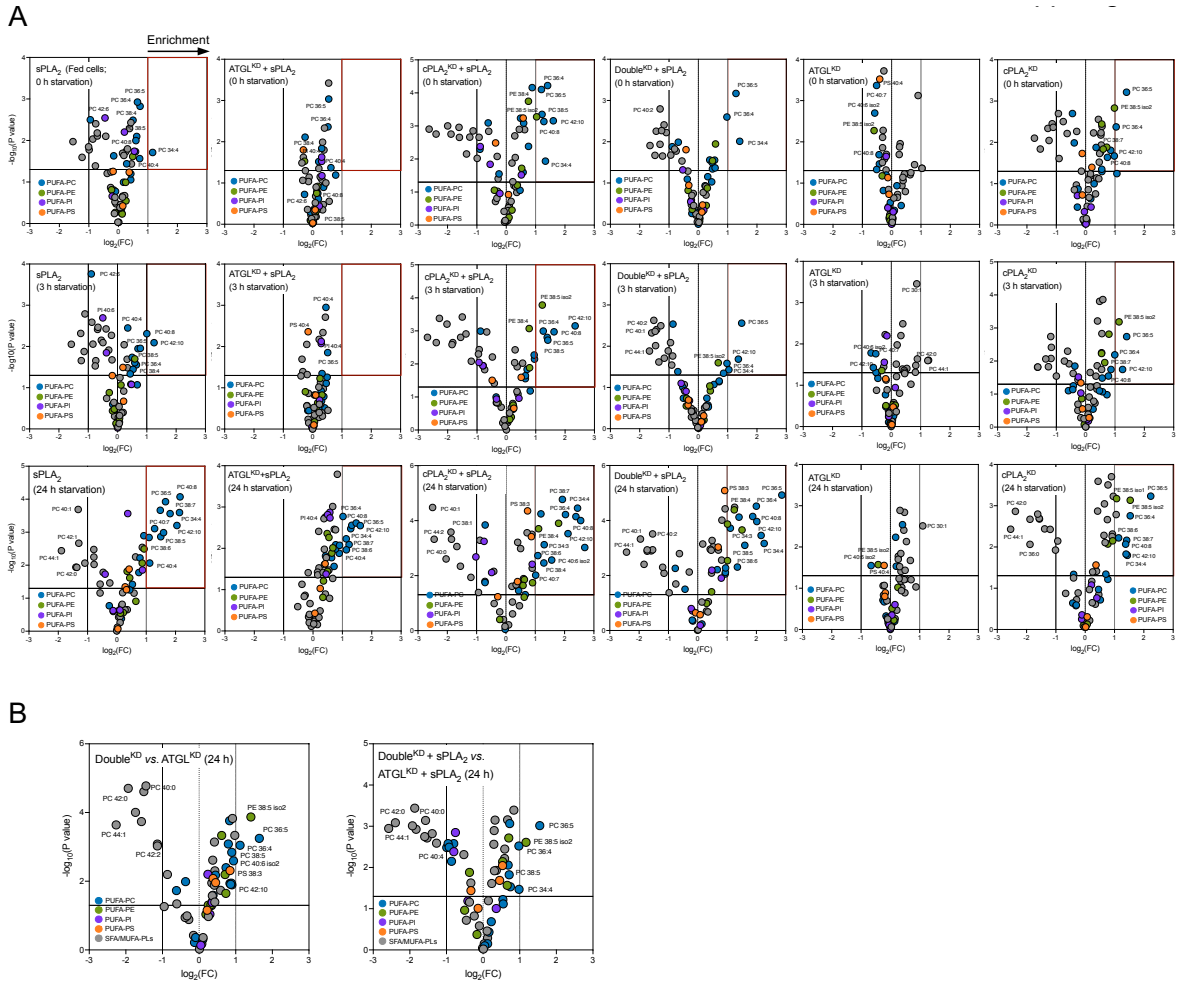

Supplementary Figure 6. Membrane phospholipid PUFA content is modulated by $sPLA_2$, $cPLA_2\alpha$ and ATGL. (**A, B**) Untargeted lipidomic analysis of phospholipids in MDA-MB-231 cells depleted of ATGL ($ATGL^{KD}$), $cPLA_2\alpha$ ($cPLA_2\alpha^{KD}$) or both ($Double^{KD}$), without and with hGX $sPLA_2$ pre-treatment, and grown as shown in (B). Volcano plots show significant changes ($-\log_{10}$(P value) > 1.30) in individual lipids between each treatment condition *versus* control cells (unless otherwise indicated), and were prepared by $\log_2$ fold-change (FC) data transformation and multiple t-test analysis (n = 3 independent experiments). Phospholipids (PLs) containing saturated and mono-unsaturated acyl chains (SFA/MUFA-PLs with 0–2 double bonds) and those containing polyunsaturated FAs (PUFA-PLs with at least 3 double bonds) are colour-coded as indicated. PC, phosphatidylcholine; PE, phosphatidylethanolamine; PI, phosphatidylinositol, PS, phosphatidylserine.

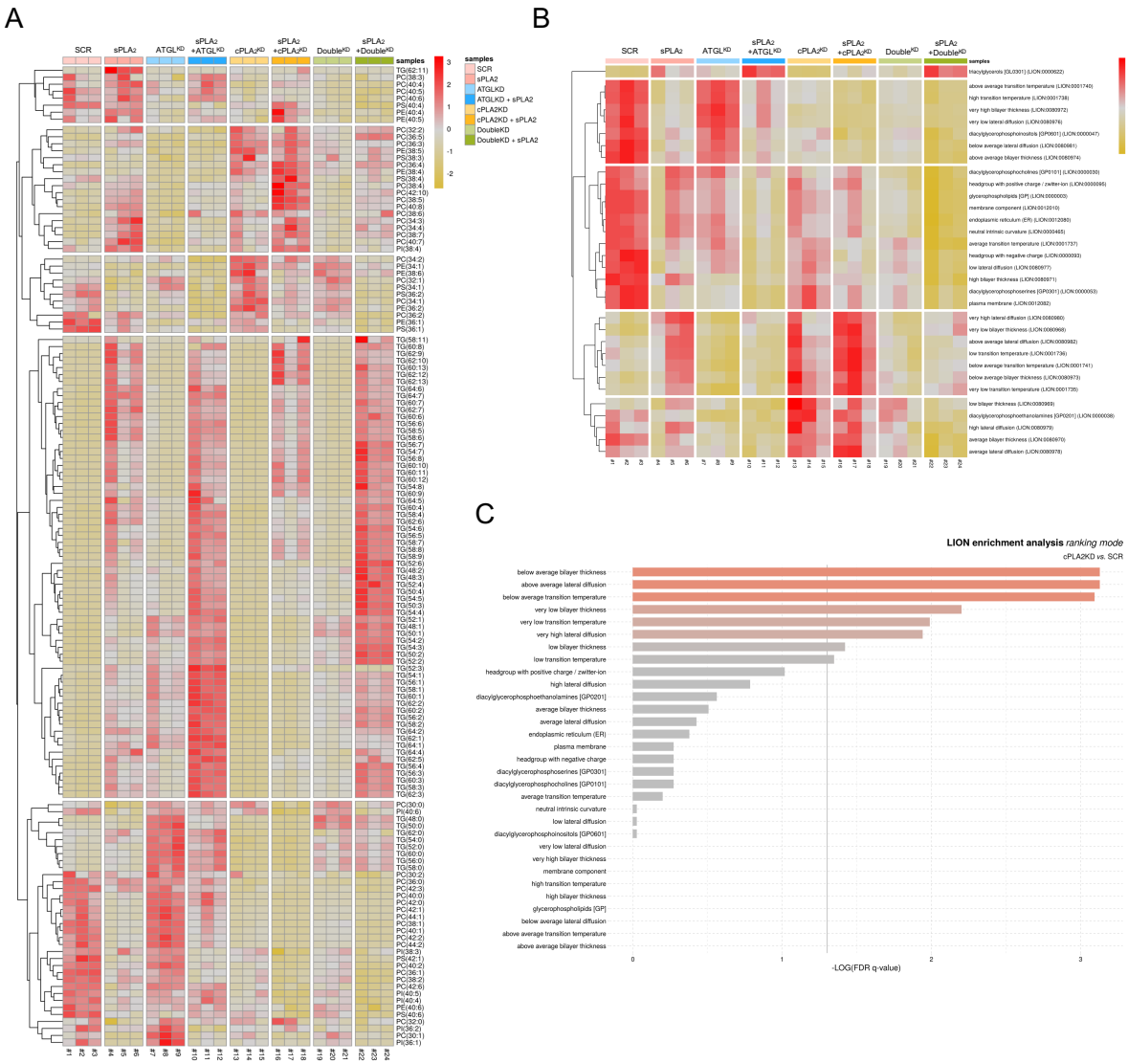

Supplementary Figure 7. LION-term enrichment analysis for significant changes in membrane properties induced by sPLA$_2$, cPLA$_2$α and ATGL. (**A**) Heat map of z-score scaled lipid levels of phospholipids and triglycerides in serum-starved MDA-MB-231 cells depleted of ATGL (ATGL^{KD}), cPLA$_2$α (cPLA$_2$α^{KD}) or both (Double^{KD}), without and with hGX sPLA$_2$ pre-treatment under serum-rich conditions. (**B, C**) LION-term enrichment analysis of the full data set (B) and pairwise comparisons of phospholipid data from cPLA$_2$α-depleted and control (SCR) cells (C) in ranking mode. The cut-off value of significant enrichments is indicated by the grey line ($q < 0.05$). Data were analysed using three principal components, and lipids were clustered into five groups by hierarchical clustering (A, B). Bar colours are scaled according to the enrichment (−log q-values). FDR, false-discovery rate.

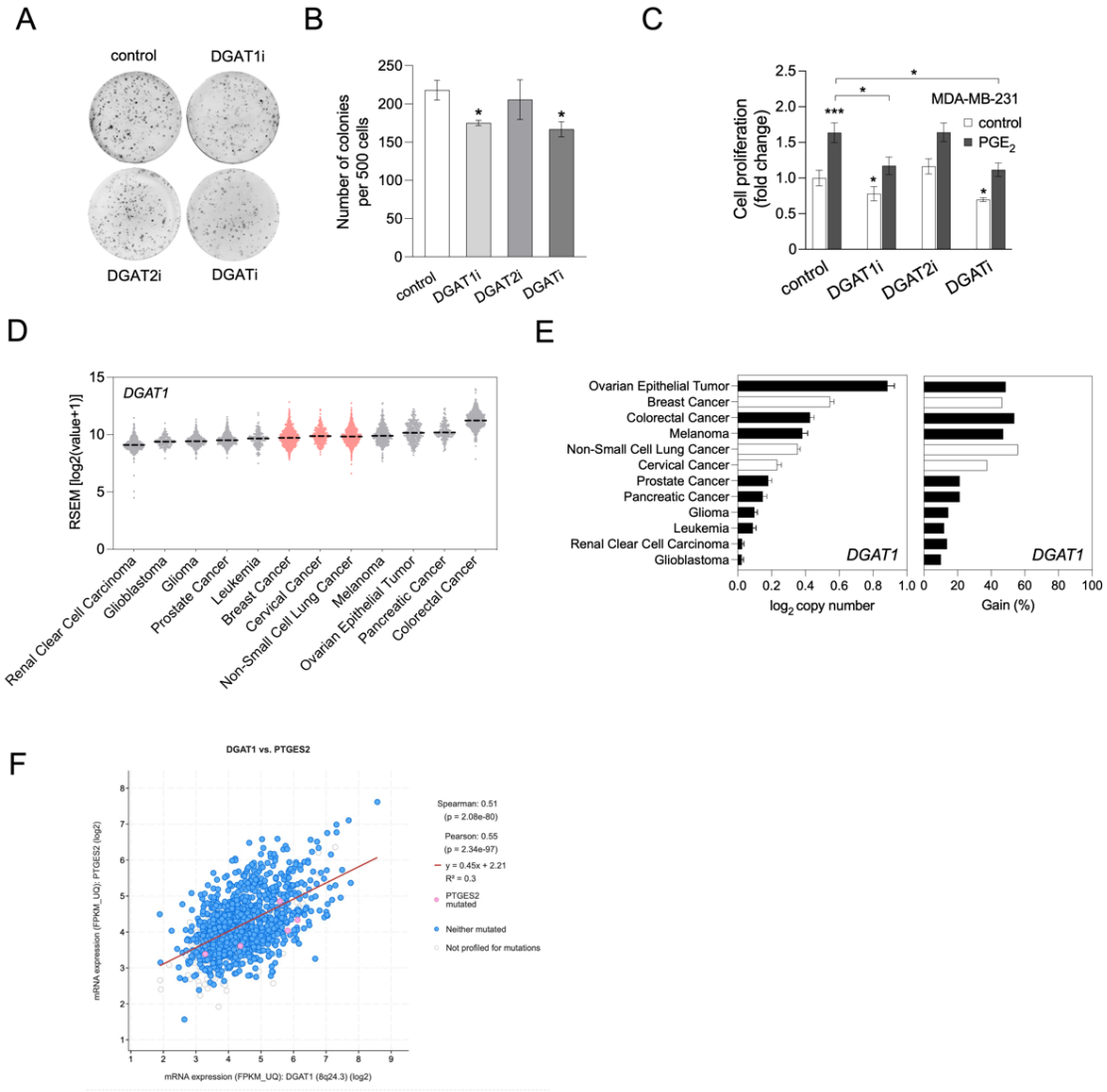

Supplementary Figure 8. The *DGAT1* is gene is upregulated in several cancers and DGAT1 inhibitors reduce colony formation and PGE_2-induced cell proliferation *in vitro*. (**A, B**) Representative images (A) and graph (B) of DGAT inhibition-induced changes in colony formation of MDA-MB-231 cells treated grown in complete medium for nine days and treated with T863 (DGAT1i) and PF-06427878 (DGAT2i), or an equimolar mix of both DGAT inhibitors (DGATi). (**C**) Proliferation of MDA-MB-231 cells treated with 1 μM exogenous PGE_2 in the absence and presence of T863 (DGAT1i) and PF-06427878 (DGAT2i), or an equimolar mix of both DGAT inhibitors (DGATi). (**D**) *DGAT1* mRNA levels in samples from cancer patients (TCGA PanCancer Atlas Studies, cBioportal). mRNA levels were batch normalized from Illumina HiSeq_RNASeqV2. Dashed line indicates median. (**E**) *DGAT1* gene copy number and gain in copy number in samples of cancer patients (TCGA PanCancer Atlas Studies, cBioportal). Gain (%) refers to the percentage increase in the number of gene amplifications beyond the diploid copy number. (**F**) Correlation between mRNA levels of *DGAT1* and *PTGES2* genes in different cancer types (TCGA PanCancer Atlas Studies, cBioportal). Spearman's rank correlation coefficient. Data are means ±SEM of three independent experiments. *, P < 0.05; **, P < 0.01; ***, P < 0.001 (unpaired t-test (B); two-way ANOVA with Tukey (C) adjustment).